Real Comparator Behavior and Its Effect on Wake-Up Receivers

Robert Fromm
Faculty of Engineering
Leipzig University of Applied Sciences
Leipzig, Germany
0000-0002-2905-0648

Olfa Kanoun
Department of Electrical Engineering and Information Technology
Chemnitz University of Technology
Chemnitz, Germany
0000-0002-7166-1266

Faouzi Derbel
Faculty of Engineering
Leipzig University of Applied Sciences
Leipzig, Germany
0000-0002-7038-8157

***Abstract*—Wake-up receivers (WuRxs) enable low-latency wireless communication with power consumption three orders of magnitude lower than that of conventional RF receivers. Most WuRxs based on commercial off-the-shelf components rely on a comparator to digitize the analog LF signal. The comparator is the central component that determines achievable WuRx sensitivity, range, and energy efficiency. High input offset voltage or large hysteresis increase the required signal amplitude and therefore degrade the minimum detectable signal (MDS). This work presents detailed measurements of comparator trip levels for eight devices, providing realistic values for input offset and hysteresis. Based on these measurements, formulas are derived to estimate the WuRx MDS from the comparator parameters and the envelope-detector voltage sensitivity. The results show that increasing the common-mode voltage can improve the MDS by up to 1.8 dB. Two comparators not previously used in WuRxs were evaluated. The ISL28915 achieves the lowest MDS of –48 dBm at only 500 nA supply current, making it suitable for always-on WuRxs. The MAX9075 offers low propagation delay and a supply current of 3 µA, providing a clear improvement over the TLV3201 previously used in duty-cycled WuRxs. These findings provide practical design guidance for comparator selection and enable improved MDS in future WuRx implementations.**

***Index Terms*—Wake-up receiver, wireless sensor network, ultra-low power, comparator, input offset voltage, hysteresis.**

I. Introduction

A long battery life of sensor nodes is essential for modern wireless sensor networks. The reception mode of a sensor node consumes most of the available energy. Continuous data reception is desirable, yet it prevents multi-year battery life [1]. Modern RF transceivers draw more than 10 mW during continuous reception, which makes duty cycling necessary to reduce power consumption. This approach increases latency in event-driven communication and limits the use of battery-powered systems in many real-time applications. [2]

One solution is the use of a specialized RF receiver called a wake-up receiver (WuRx). Typically, a WuRx has a power consumption that is lower by three orders of magnitude, at 10 µW. This low power demand allows sensor nodes to receive RF packets continuously and energy-autarkic. Most WuRx can only detect dedicated packets known as wake-up packets (WuPts). The main radio of the sensor node can be configured to generate these WuPts. [3]–[5]

Recent publications present various WuRx prototypes based on different technologies. This article focuses on WuRxs built from commercial off-the-shelf (COTS) components. These WuRxs are known for simplicity and good repeatability because all required components are widely available [3], [4], [6].

Our large-scale literature survey [7] showed that COTS WuRxs differ in the way how the analog LF signal is converted into a digital level. The surveyed prototypes use analog-to-digital converters [8], logic thresholds [9], low-frequency pattern matchers [5], or comparators [6]. Most COTS WuRxs rely on comparators.

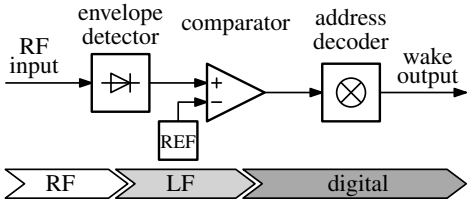

Fig. 1. Building blocks of a commercial off-the-shelf wake-up receiver based on comparator digitization. RF envelope detector performs the RF to LF conversion. Comparator digitizes the LF signal. A reference generator is required on the comparator's second input.

Additionally, most COTS WuRxs use WuPts modulated with on-off keying (OOK). This allows the use of passive radio-frequency envelope detectors (RFEDs) for down-conversion of the RF signal. The RFED is the first critical component because its voltage sensitivity defines the strength of the resulting LF signal. [4], [7]

Research funded by the German Research Foundation (DFG) under project number 466653706 as part of the project "Sensor-integrating Gear" (SIZA).

Digital circuits used for LF signal conversion are affected by the shoot-through effect. This effect increases the supply current of CMOS stages and makes such circuits unsuitable for low-power WuRxs. [9]

The comparator requires a reference generator. The different reference circuits will be discussed in the next section. Optional LF amplifiers can be placed between the RFED and the comparator to increase the signal level. In some WuRxs the output of the comparator triggers the wake-up of the sensor node. Other designs use address decoders that perform a pattern match and wake up the node only when a valid address is detected. [6], [7]

This article focuses on the selection and evaluation of suitable comparators for WuRxs. The trip levels of different devices were measured across the full common-mode voltage range to obtain realistic values for input offset voltage and hysteresis. These measurements show how input offset affects both inputs of the comparator and how with certain devices the minimum detectable signal (MDS) of the WuRx can be improved by up to 1.8 dB. The analysis includes the functional principles of several reference generators, and a formula is provided to convert the measured trip levels into a MDS of the WuRx. The study also introduces three comparators not previously used in the state of research. Two of these show promising performance for future WuRx designs. The presented measurements support a more reliable component selection process and simplify future WuRx development.

II. State of Research

A. Comparator Selection

When selecting a comparator for WuRx, four key parameters must be considered. The input offset and hysteresis define the minimum input level and affect the MDS of the WuRx. The propagation delay limits the response time and the maximum data rate of the WuRx. The quiescent supply current determines the energy demand of the comparator and contributes directly to the power budget of the WuRx.

Hysteresis improves noise suppression but reduces the MDS. The minimum signal required to switch the comparator is defined by the lower and upper trip levels. These trip levels ΔV_{T+} and ΔV_{T-}, depend on the input offset V_{OS} and the hysteresis V_{hys} [10]:

$$\Delta V_{T+} = V_{OS} + V_{hys}/2, \tag{1}$$

$$\Delta V_{T-} = V_{OS} - V_{hys}/2. \tag{2}$$

Table I summarizes the parameters of comparators suitable for WuRx applications. The first eight comparators originate from the state of research, and the last three result from an additional component search.

The TLV3691 was identified in 16 prototypes [7]. This comparator has the lowest quiescent current of 75 nA. For this reason, the TLV3691 is commonly selected for WuRxs powered by energy harvesting [11]. Magno et al. [6] reported a sensitivity of −32 dBm for a WuRx using this comparator.

TABLE I
Comparators for Wake-up Receivers

comparator	V_{OS}[1] in mV	V_{hys}[2] in mV	supply in V	current in nA	delay[3] in µs
TLV3691	±15[b]	17	0.9–6.5	75	45
AS1976	±5[e]	3	1.8–5.5	200	15
TS881	±6[b], ±10[a]	2.4	0.85–5.5	300	13
LTC1540	±12[c]	50	2.0–11.0	300	60
LPV7215	±5[d], ±6[a]	—	1.8–5.5	580	15
TLV3701	±5[b]	—	2.7–16	580	67
MAX9119	±5[e]	4	1.6–5.5	680	16
TLV3201	±3[b]	1.2	2.7–5.5	40000	0.055
ISL28915	±2[b]	—	1.8–5.5	500	260
TLV3401[4]	±3.6[b]	—	2.7–16	560	80
MAX9075	±8[a]	—	2.1–5.5	3000	0.58

Typical performance parameters from the comparator's datasheet
[1] maximum input offset voltage at room temperature
[2] typical hysteresis voltage
[3] maximum propagation delay, approximately 10 mV overdrive
[4] open drain outputs
Common-mode voltage: [a] 0 V, [b] $V_{CC}/2$, [c] 2.5 V, [d] V_{CC}, [e] full range

Other studies obtained similar values [12] or added LF amplifiers for improved sensitivity [3].

The AS1976 is no longer in production and was also used by Magno et al. [6]. This comparator offers a good balance between power consumption and sensitivity. The authors reported a sensitivity of −42 dBm for a WuRx based on this comparator.

The TS881 is a suitable replacement for the previous comparator. Hutu et al. [13] used this comparator in a WuRx capable of receiving OFDM WuPts.

The LTC1504 was used in several early WuRx designs. It provides a higher hysteresis than most other comparators and includes an integrated reference voltage of approximately 1.2 V. Ma and Paradiso [14] employed this comparator in 2002 for an optical WuRx. Marinkovic and Popovici [15] proposed an RF WuRx based on this comparator and developed logic circuits to detect the preamble of a WuPt.

The LPV7215 was identified in 16 additional prototypes during our literature survey [7]. Its main advantage is a near-zero hysteresis, which significantly reduces the trip levels. Magno et al. [6] reported a sensitivity of −55 dBm for a WuRx using this comparator. With the addition of an LF amplifier, a sensitivity of −65.8 dBm was achieved in our earlier work [3].

The TLV3701 and the MAX9119 show similar performance characteristics and were used in only a few publications [7], [16].

The TLV3201 is used in duty-cycled WuRxs where high speed is required. Bdiri et al. [17] and our earlier design [18] rely on LF values of 128 kHz and 100 kHz, respectively. These WuRxs remain active for only 50 µs, during which the presence of a WuPt on the channel must be detected. Such high LF values cannot be digitized with the microsecond-level propagation delays of the previously discussed comparators.

Based on component search, three additional comparators were identified that do not appear in previous research.

B. Reference Generator

The second component required for digitizing the LF signal is the reference signal applied to the second comparator input. The process of converting the LF signal into a digital output is commonly referred to as data slicing. Several data-slicing circuits are described in the application note [19]. Fig. 2 illustrates two typical comparator circuits used in WuRxs.

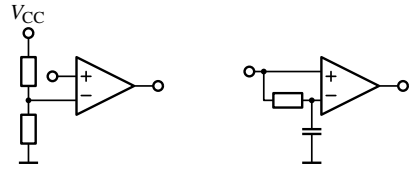

(a) fixed reference (b) adaptive reference

Fig. 2. Comparator circuits used in wake-up receivers

In Fig. 2 (a), a fixed reference voltage is generated by a resistor divider. An external reference or an internal reference, as available in comparators such as the LTC1540, can also be used. The reference levels reported in the analyzed studies range from 0.6 mV to 1 V [7]. The selection of a suitable fixed reference voltage will be discussed in the Section III.

The circuit in Fig. 2 (b) removes the need for a fixed reference by generating the reference voltage directly from the input signal. A low-pass filter averages the input signal. This approach provides two advantages. It compensates offset, because any DC offset on the input signal is corrected. It also draws no quiescent current. When the input voltage is supplied directly by a passive RFED, even the energy required to charge the capacitor is obtained passively.

The data slicer time constant τ_{DS} is defined by the product of the resistor and capacitor value. This constant determines both the responsiveness and the robustness of the data slicer. A high τ_{DS} requires a long preamble, because the reference must settle longer. A low τ_{DS} limits the run length of the WuPt [20]. Long sequences of identical symbols can saturate the data slicer and cause additional bit errors. [19].

Many articles rely on the adaptive reference generator [3], [6], [11], [15]–[18]. The functional principle, the selection of the resistor value, and the choice of the data slicer time constant are rarely discussed in these studies.

For additional robustness against noise, several studies include an external hysteresis circuit [17], [18]. This circuit uses a resistor divider to feed a fraction of the comparator output back to its input, thereby creating a defined hysteresis window.

C. Conclusion

In the last two subsections, the comparators and reference generators used in the state of research were examined. Only a fraction of the WuRx prototypes employing comparators could be listed here. We published the full list of 56 prototypes in [7]. This number highlights the importance of the comparator in WuRx design.

In Table I, the typical parameters listed in comparator datasheets were highlighted. The input offset and the hysteresis are critical parameters because they directly influence the WuRx MDS. These quantities are not constant and depend on the common-mode voltage V_{CM}. Many datasheets specify the input offset only for a single common-mode value, as indicated by the alphabetical footnotes in Table I.

The upcoming measurements will investigate the impact of the common-mode voltage on the input offset. The advantages and disadvantages of fixed and adaptive reference generators will be shown.

III. Theory

A passive RFED is assumed, which converts the RF signal at, for example, 868 MHz into an LF signal. The LF signal is treated as a square-wave that carries the address information of the WuPt [7]. For passive RFEDs based on Schottky diodes, the output voltage V_{ED} is linear with respect to the input RF power P_{RF}. This linear function holds as long as the diode operates in its square-law region. This region is generally valid for input powers below $-30\,\mathrm{dBm}$ [21, p. 568].

$$V_{ED} = \gamma P_{RF} \tag{3}$$

γ is the voltage sensitivity of the RFED and is typically around $40\,\mathrm{mV/\mu W}$ [3]. The voltage sensitivity of the RFED should be measured. If an LF amplifier is included, its gain must be incorporated into γ for the following calculations.

Based on Eq. 1 and 2, the required low and high levels of the input signal, V_{in-} and V_{in+}, can be estimated. These levels define the voltages needed to trigger the comparator in both directions. V_{ref} is the reference voltage connected to the second comparator input. In this set of conditions, the input offset V_{OS} is replaced by the worst-case minimum V_{OS-} and maximum V_{OS+} limits. Most comparator datasheets, as well as our measurements, show a symmetrical offset ($V_{OS+} = -V_{OS-}$).

$$V_{in+} - V_{ref} > V_{OS+} + V_{hys}/2 \tag{4}$$

$$V_{in-} - V_{ref} < V_{OS-} - V_{hys}/2 \tag{5}$$

For a typical RFED output, the square-wave signal is referenced to ground ($V_{in-} = 0$). Using Eq. 5 and assuming a fixed reference voltage, a condition for V_{ref} is obtained that must be satisfied for the comparator to return to its low state.

$$V_{ref} > V_{hys}/2 - V_{OS-} \tag{6}$$

This condition shows that a minimum reference voltage is required to ensure that the comparator can return to its low state after an RF pulse. For the TLV3691, with $V_{OS-} = -15\,\mathrm{mV}$ and $V_{hys} = 17\,\mathrm{mV}$, the resulting lower limit for the reference voltage is 24.5 mV.

Inserting this condition into Eq. 4 yields the input level required to trigger the comparator. Applying Eq. 3 then gives the corresponding minimum detectable RF power.

$$V_{in+} > 2 \cdot V_{OS+} + V_{hys} \tag{7}$$

For the example of the TLV3691, the resulting MDS is 49 mV. With a voltage sensitivity of $40\,\mathrm{mV/\mu W}$, the minimum

detectable RF signal is −29.1 dBm for a comparator operated with the minimum fixed reference voltage.

For the adaptive reference, ideal low-pass filtering of the square-wave input produces an average value of the signal amplitude at the second comparator input.

$$V_{\text{ref,adap}} = (V_{\text{in}+} + V_{\text{in}-})/2 \tag{8}$$

With the lower input voltage at ground ($V_{\text{in}-} = 0$) and symmetrical input offsets, Eq. 4 and 5 yield the same condition.

$$V_{\text{in}+}/2 > V_{\text{OS}+} + V_{\text{hys}}/2 \tag{9}$$

This condition matches the expression derived for the fixed reference in Eq. 7 and leads to the same MDS.

Both circuits have different disadvantages. For the fixed reference voltage, a safety margin must be added to the minimum reference level. If the reference voltage is too low and the input offset becomes strongly negative, the comparator cannot reset, and no signal reception is possible. This results in a complete malfunction of the WuRx. The reference voltage must be increased to anticipate component variations.

Secondly, the adaptive reference voltage relies on low-pass filtering of the input signal, and this filtering is not ideal. A preamble is required to cover the settling time of the data slicer. The WuPt must have a short run length and a balanced sequence of low and high symbols [7], [20]. If these conditions are not met, the reference voltage will not remain centered between the signal levels, and the sensitivity will degrade.

IV. Methodology

Based on the discussion in Subsection II-A and the parameters in Table I, the following comparators were selected for the investigations: TLV3691, AS1976, TS881, LPV7215, TLV3201, ISL28915, TLV3401, and MAX9075. The LTC1540, TLV3701, and MAX9119 were not included because their parameters were inferior to other available options. Each measurement was repeated for 3–5 devices per comparator. Devices from different manufacturing batches were included whenever possible.

The goal is to develop a measurement setup that can vary both comparator inputs and detect the trip levels. Fig. 3 shows the implemented setup.

The Rigol DG1022Z function generator was used for the measurements. Directly connecting both generator channels to the comparator inputs is not suitable, because the channel-to-channel voltage offset can exceed the input offset of the device under test. To avoid this issue, channel 1 was used to generate the small differential voltage V_1, and channel 2 was used to generate the common-mode voltage V_{CM} over a wide range. The devices under test were supplied from a 3 V battery. For this reason, V_{CM} was swept from −0.1 V to 3.1 V. Extending V_{CM} beyond the supply voltage is typical for comparators [22, p. 812]. For channel 2, the DC output mode of the function generator was used.

The differential voltage generated by channel 1 must be significantly smaller than V_{CM}. To improve the effective resolution of the function generator and the oscilloscope accuracy,

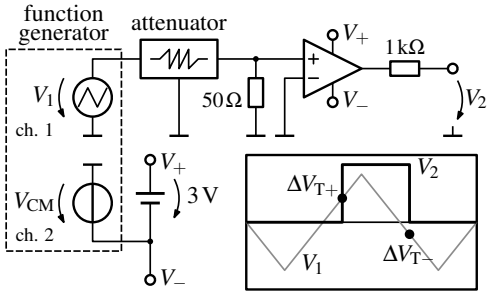

Fig. 3. Measurement setup for determining comparator trip levels. Channel 1 generates the triangle wave V_1. Channel 2 generates the inverted common-mode voltage V_{CM}. The oscilloscope measures V_1 and the comparator output V_2. The trip levels $\Delta V_{\text{T}+}$ and $\Delta V_{\text{T}-}$ are obtained by converting the values of V_1 at the level transitions of V_2.

40-dB and 60-dB attenuators were used. The maximum output voltage of the generator is limited to ±5 V, which restricts the use of the 60-dB attenuator to devices with trip levels within ±5 mV. The 40-dB attenuator was required only for the TLV3691 and the TLV3201.

Using the DC output mode on channel 1 was not possible, because changing the DC level produced spikes that could override the comparator hysteresis. A triangle signal was therefore used instead. Measurements were performed using a Rigol DS1054Z oscilloscope. The oscilloscope was triggered on the rising and falling edges of the comparator output V_2 to capture the trip levels based on the attenuated value of V_1.

The measurement error of the trip levels is mainly determined by the oscilloscope voltage accuracy and the attenuator tolerance. Although the relative error is on the order of 15%, the absolute error remains low. It is ±500 µV with the 40-dB attenuator and only ±50 µV with the 60-dB attenuator.

The frequency of the triangular wave must be chosen carefully, because a frequency that is too high introduces additional error. With a propagation delay of 100 µs and a selected frequency of 1 Hz, the resulting offset error remains below 10 µV. All experiments were performed at room temperature.

V. Results

Fig. 4 shows a typical result of a trip-level measurement. The example is taken from the second TS881 device. The trip levels shown in the plot were measured directly. Using Eq. 1 and 2, the input offset and the hysteresis were calculated and are included in the plot as well.

These measurements, like many others performed on different comparators, show a distinct step near 500 mV of V_{CM}. Several comparators also show an additional step close to 2.5 V. These steps are presumed to result from non-linearities in the input stage when the common-mode voltage approaches one diode drop.

To summarize the measurements, the input offset and the hysteresis of all comparators are plotted in Fig. 5. The key values of the comparators are listed in Table II. The table reports the mean absolute values at $V_{\text{CM}} = 0$ and the values measured in the V_{CM} range from 0.7–2.3 V. The MDS power was calculated using Eq. 3 and 9.

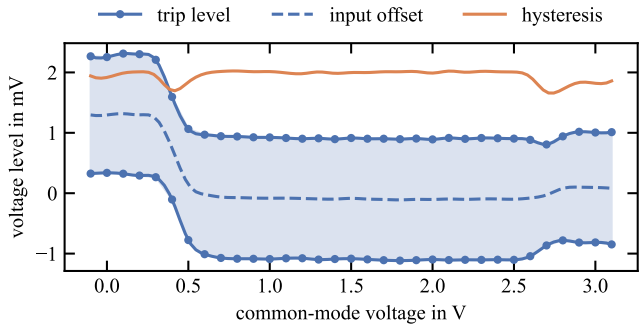

Fig. 4. Trip-level measurement of TS881 device 2. The input offset is calculated as the average of the two trip levels. The hysteresis is calculated from the difference between the trip levels.

TABLE II
SUMMARIZED MEASUREMENT RESULTS

comparator	V_{OS} in mV for $V_{CM} = 0$	V_{hys} in mV for $V_{CM} = 0$	MDS in dBm for $V_{CM} = 0$	V_{OS} in mV for $0.7\,V \leq V_{CM} \leq 2.3\,V$	V_{hys} in mV for $0.7\,V \leq V_{CM} \leq 2.3\,V$	MDS in dBm for $0.7\,V \leq V_{CM} \leq 2.3\,V$
TLV3691	3.76	21.45	−31.4	0.70	17.83	−33.2
AS1976	0.63	2.94	−39.8	1.13	2.40	−39.3
TS881	0.90	2.04	−40.2	0.52	2.10	−41.1
LPV7215	0.35	0.13	−46.9	0.35	0.13	−46.8
TLV3201	2.19	3.03	−37.3	1.31	1.70	−39.7
ISL28915	0.29	0.00	−48.4	0.27	0.00	−48.7
TLV3401	1.38	0.12	−41.4	1.38	0.12	−41.4
MAX9075	1.25	—	−42.0	1.36	—	−41.7

The TLV3691 shows the highest input offset and hysteresis in this study. Its supply current is lower by at least a factor of three compared to all other commercially available comparators. The hysteresis is stable and decreases by only 15% with increasing V_{CM}. An MDS of −31.4 dBm is reached at $V_{CM} = 0$. Increasing V_{CM} to mid-supply improves the MDS.

The AS1976 achieves a significantly better MDS of −40 dBm. It shows two steps at 0.5 V and 2.5 V. The hysteresis remains stable at 2.5 mV. Increasing V_{CM} provides no measurable advantage.

Because the AS1976 is no longer available, the TS881 serves as a suitable replacement. The measured devices show similar input offset and hysteresis levels. Increasing V_{CM} provides no benefit.

The LPV7215 offers a clear advantage in MDS because of its very low hysteresis. However, the measured MDS does not reach the −55 dBm reported by Magno et al. [6]. Our measurements show a degradation of 8 dB, while the TLV3691 and AS1976 match within 2 dB of reported values. The LPV7215 exhibits a stable hysteresis of 0.13 mV and a clear offset step at 2.5 V.

The TLV3201 is known for its fast propagation delay but has a supply current that is higher by a factor of 100. Its input offset and hysteresis are comparable to the AS1976 and TS881. It is the only comparator showing two steps in hysteresis, with values decreasing from 3 mV to 1.7 mV. This comparator therefore benefits from increasing V_{CM}.

The ISL28915 has a supply current of only 500 nA and reaches the lowest MDS in this study. The measured hysteresis is below the resolution and the input offset is very low. An MDS of −48 dBm is achieved without additional amplification. This comparator justifies further investigation because its MDS is excellent and its supply current is even lower than that of the LPV7215.

The TLV3401 provides no clear benefit compared to the AS1976 or TS881. Its MDS is only slightly improved, while its supply current is nearly doubled. Because it has open-drain outputs, it may require extra power from a pull-up resistor.

With the MAX9075, no hysteresis could be measured. Its internal hysteresis is so low that noise on the triangular input produced multiple output transitions. The positive trip level was measured at the first observable transition. Due to its short propagation delay and a supply current of 3 µA, this comparator is suitable for fast duty-cycled WuRxs. It offers clear advantages over the TLV3201, previously used for duty-cycled designs [17], [18], in terms of MDS, supply current, and supply voltage range.

VI. CONCLUSION

Comparators play a central role in wake-up receivers (WuRxs) because their input offset voltage, hysteresis, propagation delay, and supply current directly determine the achievable sensitivity, data rate, and energy consumption of the WuRx. Their behavior defines the minimum detectable signal (MDS) and thus sets the fundamental performance limits of comparator-based WuRx architectures.

The theoretical calculations presented in this work show the conditions required for reliable switching of the comparator. A fixed reference voltage carries the risk of WuRx malfunction when the reference is set too low and the input offset becomes strongly negative. An adaptive reference avoids this problem but introduces a run-length limit, as long sequences of identical symbols in the WuPt can shift the reference level and degrade the WuRx sensitivity.

The measurement results reveal the true variation in the input offset voltage between the different comparator devices (see Fig. 5). Additionally, there are distinct steps in the input offset, typically near a common-mode voltage of 0.5 V and 2.5 V. These steps affect the trip levels and the WuRx MDS. The results also show that increasing the common-mode voltage can improve MDS by up to 1.8 dB for specific comparators.

Two comparators not previously used in the state of research were evaluated, and both show clear advantages. One comparator offers excellent MDS with very low supply current, and the other provides fast switching performance suitable for duty-cycled WuRxs while keeping power consumption low.

Overall, the theoretical analysis and measurement results provide a clear foundation for selecting suitable comparators and reference generator circuits for future WuRx designs. The presented investigation is limited to room temperature. Future work will include experiments assessing comparator operation and overall WuRx performance across a wider temperature range.

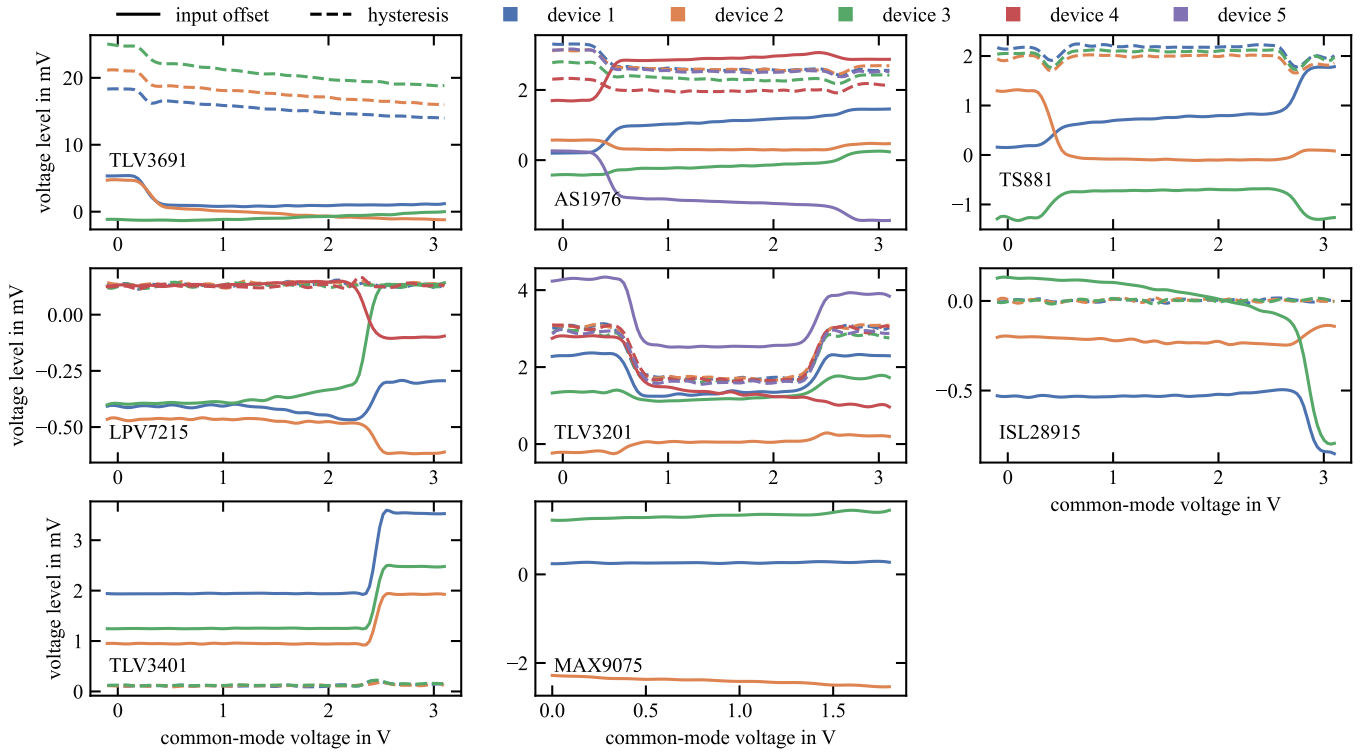

Fig. 5. Input offset and hysteresis of all measured comparators. No hysteresis was measured for the MAX9075 because it was significantly lower than the resolution of the measurement setup.

Data Availability Statement

The data presented in this study are openly available in FigShare at 10.6084/m9.figshare.30800636.

References

[1] J. Braun and F. Derbel, "Wireless sensor network for fire detection with network coding to improve security and reliability," *Measurement: Sensors*, 2024.

[2] O. Kanoun, S. Bradai, S. Khriji, G. Bouattour, D. El Houssaini, M. Ben Ammar, S. Naifar, A. Bouhamed, F. Derbel, and C. Viehweger, "Energy-aware system design for autonomous wireless sensor nodes: A comprehensive review," *Sensors*, vol. 21, no. 2, 2021.

[3] R. Fromm, L. Schott, and F. Derbel, "Improved wake-up receiver architectures with carrier sense capabilities for low-power wireless communication," in *Sensor Networks*, A. Ahrens, R. V. Prasad, C. Benavente-Peces, and N. Ansari, Eds. Cham: Springer International Publishing, 2022, pp. 60–84.

[4] R. Piyare, A. L. Murphy, C. Kiraly, P. Tosato, and D. Brunelli, "Ultra low power wake-up radios: A hardware and networking survey," *IEEE Communications Surveys Tutorials*, vol. 19, no. 4, pp. 2117–2157, 2017.

[5] G. U. Gamm, S. Stoecklin, and L. M. Reindl, "Wake-up receiver operating at 433 MHz," in *2014 IEEE 11th International Multi-Conference on Systems, Signals Devices (SSD14)*, 2014, pp. 1–4.

[6] M. Magno and L. Benini, "An ultra low power high sensitivity wake-up radio receiver with addressing capability," *International Conference on Wireless and Mobile Computing, Networking and Communications*, pp. 92–99, Nov. 2014.

[7] R. Fromm, O. Kanoun, and F. Derbel, "Wake-up receivers based on commercial off-the-shelf components: a survey," *IEEE Journal of Microwaves*, vol. 6, no. 1, pp. 42–80, 2026.

[8] T. Ma, "A bit sampled wake-up receiver with logarithmic detector architecture," in *2017 International Conference on Cyber-Enabled Distributed Computing and Knowledge Discovery (CyberC)*, 2017, pp. 445–449.

[9] R. Fromm, O. Kanoun, and F. Derbel, "The necessity of comparators in wake-up receiver circuits," in *2024 21st International Multi-Conference on Systems, Signals & Devices (SSD)*, 2024, pp. 480–485.

[10] "TLV3691 0.9-V to 6.5-V, Nanopower Comparator," Texas Instruments, Nov. 2015, datasheet.

[11] D. Fabbri, A. Romani, A. Costanzo, and D. Masotti, "An orientation-independent uhf battery-less tag for extended-range applications," in *2020 XXXIIIrd General Assembly and Scientific Symposium of the International Union of Radio Science*, 2020.

[12] A. A. Benbuk, N. Kouzayha, J. Costantine, H. Jaafar, and Z. Dawy, "A nano-watt dual-mode address detector for a Wi-Fi enabled RF wake-up receiver," in *2019 IEEE SENSORS*, 2019.

[13] F. Hutu, D. Kibloff, G. Villemaud, and J. Gorce, "Experimental validation of a wake-up radio architecture," in *2016 IEEE Radio and Wireless Symposium (RWS)*, 2016, pp. 155–158.

[14] H. Ma and J. A. Paradiso, "The FindIT flashlight: Responsive tagging based on optically triggered microprocessor wakeup," in *UbiComp 2002: Ubiquitous Computing*, G. Borriello and L. E. Holmquist, Eds. Berlin, Heidelberg: Springer Berlin Heidelberg, 2002, pp. 160–167.

[15] S. Marinkovic and E. Popovici, "Nano-power wireless wake-up receiver with serial peripheral interface," *Selected Areas in Communications, IEEE Journal on*, vol. 29, pp. 1641–1647, Oct. 2011.

[16] T. Polonelli, M. Magno, V. Niculescu, L. Benini, and D. Boyle, "An open platform for efficient drone-to-sensor wireless ranging and data harvesting," *Sustainable Computing: Informatics and Systems*, vol. 35, p. 100734, 2022.

[17] S. Bdiri, F. Derbel, and O. Kanoun, "A tuned-RF duty-cycled wake-up receiver with -90 dBm sensitivity," *Sensors*, vol. 18, no. 1, 2018.

[18] R. Fromm, O. Kanoun, and F. Derbel, "Reliable wake-up receiver with increased sensitivity using low-noise amplifiers," in *2022 19th International Multi-Conference on Systems, Signals & Devices (SSD)*, 2022, pp. 1523–1528.

[19] "Data slicing techniques for UHF ASK receivers," Maxim Integrated, Dec. 2005, application Note 3671. [Online]. Available: https://pdfserv.maximintegrated.com/en/an/AN3671.pdf

[20] R. Fromm, O. Kanoun, and F. Derbel, "Univocal and reliable addressing

patterns for wake-up receivers based on low-frequency pattern matchers," *IEEE Sensors Journal*, vol. 24, no. 8, pp. 13 431–13 438, 2024.
[21] I. Bahl and P. Bhartia, *Microwave Solid State Circuit Design*. New York: Wiley, 2003.
[22] P. Horowitz and W. Hill, *The Art of Electronics*, 3rd ed. USA: Cambridge University Press, 2015.